Assessing sinus aerosol deposition: benefits of SPECT-CT imaging

Lara Leclerc, Jérémie Pourchez, Nathalie Prevot, Laurent Vecellio, Sandrine Le Guellec, Michèle Cottier, Marc Durand

Assessing sinus aerosol deposition: benefits of SPECT-CT imaging

Lara Leclerc[a,b,c], Jérémie Pourchez[b,c], Nathalie Prevot[a,c,d], Laurent Vecellio[e,f], Sandrine Le Guellec[e,f], Michèle Cottier[a,c], Marc Durand[a,c,g]

a Université Jean Monnet, LINA EA 4624, Université de Lyon, F-42023, Saint-Etienne, France

b Ecole Nationale Supérieure des Mines, CIS-EMSE, LINA EA 4624, F-42023 Saint-Etienne, France

c SFR IFRESIS, F-42023, Saint-Etienne, France

d CHU de Saint-Etienne, Nuclear Medicin department, F-42055, Saint-Etienne, France

e Centre d'Etudes des Pathologies Respiratoires INSERM U1100/EA 6305, Faculté de Médecine, Université François Rabelais, Tours, France

f DTF Aerodrug, Faculté de Médecine, Université François Rabelais, Tours, France

g Centre Hospitalier Emile Roux, ENT department, F-43012, Le Puy en Velay, France

ABSTRACT

Purpose: Aerosol inhalation therapy is one of the methods to treat rhinosinusitis. However the topical drug delivery to the posterior nose and paranasal sinuses shows only limited efficiency. A precise sinusal targeting remains a main challenge for aerosol treatment of sinus disorders. This paper proposes a comparative study of the nasal deposition patterns of micron

and submicron particles using planar gamma-scintigraphy imaging *vs.* a new 3-dimensional (3D) imaging approach based on SPECT-CT measurements.

Methods: Radiolabelled nebulizations have been performed on a plastinated model of human nasal cast coupled with a respiratory pump. First, the benefits provided by SPECT-CT imaging were compared with 2D gamma-scintigraphy and radioactive quantification of maxillary sinus lavage as reference for the sonic 2.8 µm aerosol sinusal deposition. Then, the impact on nasal deposition of various airborne particle sizes was assessed.

Results: The 2D methodology overestimates aerosol deposition in the maxillary sinuses by a factor 9 whereas the 3D methodology is in agreement with the maxillary sinus lavage reference methodology. Then with the SPECT-CT approach we highlighted that the higher particle size was mainly deposited in the central nasal cavity contrary to the submicron aerosol particles (33.8 ± 0.6% of total deposition for the 2.8 µm particles vs. 1 ± 0.3% for the 230 nm particles).

Conclusion: Benefits of SPECT/CT for the assessment of radiolabelled aerosol deposition in rhinology are clearly demonstrated. This 3D methodology should be preferentially used for scintigraphic imaging of sinusal deposition in Human.

Keywords: aerosoltherapy, aerosol deposition, SPECT/CT imaging.

Corresponding author at:

Lara Leclerc

Laboratoire Interdisciplinaire d'étude des Nanoparticules Aérosolisées (LINA – EA 4624)

Faculté de Médecine Jacques Lisfranc, Université Jean Monnet

15 rue Ambroise Paré, 42023 Saint-Etienne cedex 2, France

Telephone / Fax number: + 33 4 77 42 14 43 / +33 4 77 42 14 94, mail: lara.leclerc@univ-st-etienne.fr or leclerc@emse.fr

1. Introduction

The treatment of nasal infections can be challenging (Baroody, 2007; Fokkens et al., 2012). Delivering antibiotics by aerosol straight through the site of infection is a common strategy (Costantino et al., 2007). Different regions are targeted for these pathologies: the middle meatus as the major site of drainage for sinuses, the maxillary and ethmoid sinuses and the superior and posterior region of the central nasal cavity (Laube, 2007).

Thanks to ongoing development of medical technology, medical imaging has been increasingly used in respiratory research. Deposition studies are essential in the field of aerosols. Nowadays, one of the main experimental methodologies proposed in the literature consist in using radioactive aerosol associated with 2-dimensional (2D) gamma-scintigraphy imaging (Möller et al., 2011; Vecellio et al., 2011). Indeed, nuclear medicine is commonly used to determine the aerosols deposition patterns. Gamma scintigraphy uses radiolabelled formulations with gamma-ray emitting radionucleides. Different ventilation markers can be used such as Diethylene-Triamine Penta-Acetic Acid (DTPA) labeled with Technetium 99m (^{99m}Tc), ^{81m}Krypton gas or Technegas. The distribution of the radioactive aerosol is generally assessed by a single-head gamma scintigraphy. However, planar gamma camera imaging provides 2D nuclear data without any visualization of anatomical features such as maxillary sinuses (Möller et al., 2008, 2010a, 2010b; Moller et al., 2011; Vecellio et al., 2011).

Currently, SPECT is a 3D imaging modality routinely used in clinical nuclear medicine. The 3D informations implement other methods in airway research by giving topographical informations, visualization of functional or structural modifications, a sampling of the whole organ and potential for *in vivo* imaging in a repeated prospective nature. In research field, 3D imaging techniques (e.g. SPECT) have the potential to give more detailed data on regional aerosol deposition. Over the last few years combined SPECT-CT scanners have become available. The concomitant acquisition without moving the patient and on the

same equipment improves the alignment. The combination of SPECT and CT enables us to assess regional function in relation to structural changes and so the action ways of drugs in airway diseases. Clinically, SPECT has considerably improved 2D measurement of radioactive aerosol deposition. The applications are very wide in the development of therapeutic aerosols and in the investigation of mucociliary clearance particularly for bronchiectasis or cystic fibrosis (Eberl et al., 2001, 2006; Fleming et al., 2011; King, 2011).

In the first part, this paper presents an innovative 3D-imaging approach using SPECT-CT compared to 2D gamma-scintigraphy and radioactive quantification of maxillary sinus lavage. Experiments were performed using a ventilated realistic plastinated nasal cast and an air-jet nebulizer generating 2.8 µm airborne particle size to accurately determine the potential benefits provided by SPECT-CT compared to planar scintigraphy. In a second part, nasal and sinus deposition were described for different sizes of aerosols using SPECT-CT imaging. The combination to CT scans accurately relates 3D nuclear images to anatomy. Thus, the impact of aerosol size and then acoustic frequency on the regional depositions especially in the different sinusal compartments was accurately evaluated.

2. Materials and methods

2.1 Plastinated nasal model and aerosol inhalation

Experiments were performed using a human plastinated nasal cast obtained by a specific plastination technique (Croce et al., 2006; Durand et al., 2001). The specimen has been obtained from a deceased man who donated his body to the Saint-Etienne Anatomy Laboratory in accordance with law and ethics committee. The obtained nasal casts do not present significant tissue retraction, the mucosa in particular is conserved. This specimen is dedicated to functional studies and has been anatomically and aerodynamically validated in a previous study (Durand et al., 2011a).

The plastinated nasal cast is ventilated as close as possible to *in vivo* conditions. A respiratory pump (Pari GmbH, Compas II) allowed us to simulate *in vivo* aerosol administration, *i.e.* a nasal inhalation and then mouth exhalation. As a compromise, the breathing parameters chosen correspond to male adult physiology at rest (breathing rates of 15 per minute, tidal volume (Vt) of 500 mL, inspiratory-to-expiratory time I/E ratio of 2/3, ET deadspace of 21 ml, tracheal diameter of 1 cm, principal bronchus diameter of 0.8 cm) (Booker, 2009; Criée et al., 2011; Flesch and Dine, 2012). A specific one-way valve simulating the soft palate (resistance = 0.13 ± 0.07 cm H_2O/min/L, mean ± SD measured for flow rates of 1 to 15 L/min) was connected to a T-piece equipped with an absolute filter, a tube 15 cm long tube simulating the trachea, and a second absolute filter. The whole mecanism was placed between the model and the pump as shown on the experimental set-up (Figure 1).

The plastinated nasal cast allowed free exterior access to the maxillary sinuses (via the cheeks, zygomatic and maxillary bones) to assay the nebulized drug deposited using maxillary sinus lavage as previously described (Durand et al., 2011b). During the inhalation experiments, two movable plastic plates were used to hermetically close the exterior access of both maxillary sinuses.

2.2 Nebulization systems

Commercial jet medical nebulizers are used to generate micrometric and submicrometric aerosols. These nebulizers are an Atomisor NL11 (DTF Medical, France), a modified Sidestream (Philips Respironics, Ref 12NEB400, England), and a Nanoneb (DTF Medical, France) operating at a flow rate of 6 $L.min^{-1}$.

The nebulization system is associated with an AOHBOX air source compressor ATOMISOR AUTOSONIQUE BOX (Diffusion Technique Française, DTF Medical, Saint-Etienne, France). During nebulization with the NL11 device, a discontinuous 100 Hz acoustic airflow

can be added to the aerosol (NL11S). The different nebulizers are connected to a nasal plug (C28 medium size, DTF Medical, France) usually employed in clinical practice. This plug ensures the interface connection between nebulizer and plastinated cast's nostrils.

The aerosol size measurement was conducted with sodium fluoride (NaF; 2.5 wt%; 4 mL), a chemical tracer recommended by European standard procedure (NF EN 13544-1) using an Electrical Low Pressure Impactor (ELPI, Dekati Ltd., Finland) as described in a previous study (Durand et al., 2011b).

2.3 Aerosol deposition

To emphasize the potential benefits of SPECT-CT, two nuclear imaging methodologies were performed to assess nasal and sinus deposition:

- Planar scintigraphy with a single-head gamma camera associated with a previous gas ventilation study using 81mKr to determine Regions Of Interest (ROIs) (Möller et al., 2008; Vecellio et al., 2011).

- 3D aerosol deposition using SPECT/CT imaging.

For the methodologies comparison, experiments were performed with the 2.8 µm aerosol with 100 Hz acoustic airflow (NL11S).

To evaluate the deposition patterns, the other types on nebulizers were compared using only the 3D imaging approach (2.8 µm NL11/NL11S, 550 nm Sidestream and 230 nm Nanoneb).

2.3.1 Assessing aerosol deposition by 2D imaging

Gamma camera imaging and 99mTc-DTPA aerosol deposition

For each experiment, NL11S nebulizers were loaded with 74MBq/3mL of 99mTc-DTPA (TechneScan DTPA, Diethyl-Triamine-Penta-Acetic acid, Mallinckrodt Medical, Petten, Netherlands); the duration of nebulization was limited to 10 min. The scintigraphic images

were recorded with a planar gamma camera (resolution 128x128) using a single detector equipped with a low-energy, high-resolution collimator: E-cam camera (Siemens, Germany - 397mm x 500mm collimator), tested monthly for uniformity (UFOV 357mm x 475mm, CFOV 268mm x 356mm). Ventilation scintigraphy was performed before the aerosol administration to precisely define three different ROIs: central nasal cavity, ethmoid and maxillary sinuses regions. 81mKr gas (81Rb-81mKr generator, Covidien, Petten, The Netherlands) was continuously administered through the nostrils of the plastinated nasal cast to measure the nasal cavity ventilation. Three images were acquired during 2 min of gas ventilation: (1) a lateral view of the nasal cavities to determine central nasal cavity and ethmoid regions; (2) a coronal section of the nasal cavities and (3) a coronal section of the nasal cavities, using an addition of 100Hz sound (AOLH box compressor) during gas administration to determine the maxillary sinus region.

Before aerosol inhalation, the initial radioactive amount charged in the nebulizer was quantified (scintigraphy image acquired over a 1-min period). After aerosol inhalation, the following images of the plastinated nasal cast were acquired over a 2-min period: (1) a lateral view showing aerosol deposition in the nasal cavities; (2) a coronal view showing deposition in the central nasal cavity and maxillary sinuses. The ROIs were defined from the ventilation images using Siemens software for the central nasal cavity, and ImageJ software (ImageJ 1.43U, National Institutes of Health, USA) for ethmoid and maxillary sinuses. The ethmoid region was defined as the upper half of the nasal region (lateral image), and the maxillary sinuses were defined as the regions seen from the coronal view (Vecellio et al., 2011). These ROIs were then applied to aerosol images to determine the radioactivity deposited in each region (nasal, ethmoid and maxillary sinus regions). The activity thus measured in the three ROIs was expressed in terms of the activity loaded into the nebulizer. All calculations also took into account the background radiation and physical decay of radioactivity.

Aerosol distribution in the nasal anatomical regions

The gamma camera images were analyzed using ImageJ software. The distribution of the aerosol deposited in the nasal anatomical regions was analyzed along three axes: the x-axis from the nostrils to the cavum, the z-axis from the floor to the upper nasal cavities, and the y-axis from the septum to the extremity of the maxillary sinuses. Distributions were normalized taking into account the pixel size and counted radioactivity. Statistical analyses were performed using StatXact® software (StatXact-3 3.0.2, Cytel Software Corporation, France). Non-parametric stratified Normal Score tests were used to compare deposition data for the three anatomical regions (central nasal cavity, ethmoid and maxillary sinuses). Strata (n=2) were determined by both nebulizers.

2.3.2 Assessing aerosol deposition by a maxillary sinus reference rinsing method

After a 2D image acquisition, the aerosol deposited in the maxillary sinuses of the plastinated nasal cast was also analyzed by radioactive counting using a rinsing method: the right and left maxillary sinuses were rinsed with 1 mL of distilled water; the liquid was collected in microtubes and the activity was counted (1 min) using an ISOCOMPT I gamma counter (MGM instruments, Hamden, USA). The activity deposited in the maxillary sinuses was expressed as a percentage of the nebulizer charge (measured with gamma camera). All calculations took into account background radiation, the physical decay of radioactivity, calibration and extraction factors. Maxillary sinus deposition data (dosages) were analyzed with Wilcoxon Mann-Whitney tests.

2.3.3 Assessing aerosol deposition by 3D imaging

Gamma camera imaging and 99mTc-DTPA aerosol deposition

SPECT generate a 3D description of a gamma-emitting radionuclide distribution using the data obtained from a rotating gamma camera. SPECT images were improved by the addition of anatomical image data. To increase the accuracy of the radioactivity distribution, the counts detected by the gamma camera were corrected for tissue attenuation improving the quality of quantification. SPECT and CT acquisitions were performed with a SYMBIA T2 variable angle dual detector SPECT with a 2-slice spiral CT for rapid accurate attenuation correction and anatomical mapping (SIEMENS, Knoxville, TN, USA).

Nebulizers were filled with 400 megabecquerels (MBq) of DTPA-Technetium 99m (^{99m}Tc) solution (DTPA Technecsan®, COVIDIEN-Mallinckrodt, ND) in a 4 mL syringe. The aerosolized fraction was evaluated for each nebulizer. Immediately after aerosol administration, each element was successively set up on the examining table in the center of the gamma cameras field. Planar images were obtained for the syringe (60-sec anterior/posterior), the nebulizer, the pulmonary filter, all accessory materials and the plastinated model (180-sec anterior/posterior). The background noise on planar images (256*256 image matrix, zoom 1) was reduced and suitable corrections were made to take into account the radioactive decay and the attenuation of gamma rays by tissues. Images obtained for the syringe, the nebulizer and the accessories were used to evaluate the quality control of nebulization experiment. We confirmed for each experiment that the total radioactivity deposited well corresponds to the total radioactivity nebulized.

Without moving the plastinated nasal cast, a 3D SPECT acquisition was performed with 64 projection (2*32) images each of 30 seconds. Finally a CT was performed with the following parameters: 130 kV, 90 mAs, slice thickness 1.25 mm, increment 0.9 mm, pitch 1.6, rotation time 1.5 s. A multimodality computer platform (Symbia net; Siemens) was used for image review and manipulation. Both the transmission and emission scans were reconstructed using 3D OSEM (8 subsets, 5 iterations), with a pre reconstruction smooth

using a 3D Butterworth filter (cutoff: 0.45 cycles/cm; order 5), 128×128 image matrix, zoom 1.23 and pixel size of 3.9 mm. SPECT images were reconstructed using scatter correction (scatter energy window) and CT attenuation correction. CT and SPECT images were matched and fused into transaxial images. Different 3D regions of interest (ROI) are manually drawn on the CT images with the software: right maxillary sinus, left maxillary sinus, frontal sinuses, ethmoid sinuses, central nasal cavity and the global head. The nuclear activity was quantified in each 3D ROI. A qualitative evaluation of the deposition is also performed by a qualified Nuclear Medicine specialist. The nuclear activity hot spot is assessed on images.

3. Results

3.1. Aerosol properties and experimental set-up

The different types of nebulizers used in this study lead to different mass median aerodynamic diameters, respectively expressed with their geometric standard deviation (± GSD): 2.8 ± 3.2 µm for the NL11/NL11S, 550 ± 2.1 for the Sidestream and 230 ± 1.6 nm for the Nanoneb. The nebulizer output rates were also assed after 10 minutes of nebulization and expressed in percentage. Respectively 0.32 ± 0.03 for the Nanoneb, 1.11 ± 0.56 for the Sidestream and 10.28 ± 1.76 for the NL11S (7.71 ± 1.24 for the NL11). The 100Hz acoustic airflow efficiently enhanced this aerosolized fraction for the micrometric aerosol. The Sidestream aerosolized fraction was three times higher than that of the Nanoneb and eight times under the aerosolized fraction of the NL11.

The experimental set-up is shown on Figure 1. A quality control of each experiment was performed by radioactive counting of planar images obtained: the initial radioactivity load in the nebulizer before the nebulization experiment; the nasal cast, the nebulizer and accessories after the nebulization). We confirmed that the total radioactivity nebulized corresponds to the total radioactivity deposited in the set-up. Only a very low radioactivity loss, fewer than 6%

of the radioactive amount introduced initially into the nebulizer, was observed during the experiments (4 ± 2%). These data assess a good reproducibility of the aerosol deposition experiments.

3.2. Aerosol deposition: 2D vs. 3D imaging

The ROI determined by 2D imaging allows us only to discriminate ethmoid region and maxillary sinuses regions *vs.* nasal deposition. The precise definition of these 2D ROI was explained in a previous study (Vecellio et al., 2011). Even if this methodology takes into account the x, y and z directions, the ROIs have approximate outlines without detailed anatomical precisions.

The definition of the 3D anatomical ROI determined by CT scans with radioactivity counting by SPECT was exposed in Figure 2A and B. With this methodology the ROIs outlines exactly correspond to the 3D scan anatomical visualization especially for the maxillary sinuses, frontal sinuses and central nasal cavity (Fig. 2A). Only the ethmoid sinuses delimitation is difficult due to the proximity of the central nasal cavity (Fig. 2B) but more realistic than in the 2D description.

For the methodologies comparison, experiments were performed with the 2.8 µm aerosol with 100 Hz acoustic airflow (NL11S). The deposited fractions are presented in Table I for the 2D and 3D approaches. Results are expressed in terms of percentage of the radioactive amount introduced initially into the nebulizer. The aerosol deposition in the maxillary sinuses was compared to the reference maxillary sinus rinsing method. The radioactivity was detected in all sinusal liquids collected after 2D acquisition of images and was quantified as percentage of the radioactive amount introduced initially into the nebulizer. We emphasized a deposition of 0.03% ± 0.02 in the maxillary sinuses of the plastinated nasal cast after nebulization for the

reference lavage. This amount of aerosol deposited in the maxillary sinuses was significantly lower than that predicted by the 2D image-processing method ($p<0.05$) which predicted 9.3 times more aerosol deposited in maxillary sinuses than the *in situ* rinsing method (0.1% ± 0.1 *vs.* 0.03% ± 0.002). However this amount is statistically equivalent to the deposition predicted by the SPECT-CT (0.03 ± 0.004% vs. 0.03% ± 0.002). This result confirms that the quantification of intrasinus deposition obtained using SPECT-CT is in agreement with the reference lavage method whereas the 2D planar scintigraphy methodology over-estimates deposition in maxillary sinuses. This over-estimation with the 2D methodology was also confirmed for the deposition in the central nasal cavity and ethmoid region (3.2 ± 0.3 *vs.* 2.38 ± 0.3 and 0.5% ± 0.1 *vs.* 0.03% ± 0.01 respectively).

3.3. Aerosol deposition in nasal anatomical regions assessed by SPECT/CT

Different types of nebulizers which have different aerosol metrologies were compared using SPECT/CT methodology: 230 nm for the Nanoneb, 550 nm for the Sidestream and 2.8 µm for the NL11. A 100 Hz acoustic effect was also assessed for the 2.8 µm particles (NL11S).

Representative images of SPECT/CT (sinusal deposition) obtained for the different nebulizers are shown on Figure 3. It clearly demonstrates a huge deposition of aerosol in the central nasal cavity for the 2.8 micrometric aerosol (NL11 device) whereas the deposition was reduced in the case of submicrometric aerosol particularly for the 230 nm aerosol (Nanoneb). The acoustic frequency enhances the deposition into the maxillary sinuses where hot spot were found with the 2.8 µm aerosol (NL11S). In the right maxillary sinus, a deposition of 0.166 ± 0.042 was found without sound vs. 0.224 ± 0.036 with a 100 Hz acoustic frequency.

ROI were traced in order to quantify the deposition as already explained (Fig. 2). The CT images allowed a precise definition in 3D of the left and right maxillary sinuses, the ethmoid sinuses, the frontal sinuses and the central nasal cavity. The main difficulty

encountered was the precise delimitation of the ethmoid region as shown on Figure 2B. A ratio was established with the global deposition in the entire plastinated nasal cast and results were presented in Figure 4 expressed as percentage of total deposition. The percentage of total deposition in the central nasal cavity was significantly higher for the 2.8 µm aerosol (33.8 ± 0.6%) while deposition was reduced for the 550 and 230 nm aerosol (respectively 1.3 ± 0.1% and 1 ± 0.3%). Only small amount of radioactivity was quantified in the other anatomical regions. Indeed, less than 1% of the total aerosol deposition was detected in the maxillary and ethmoid sinuses and non significant values in the frontal sinuses. However it clearly demonstrates a significant efficiency of the acoustic frequency of the NL11 nebulizer (2.8 µm) to enhance aerosol deposition in the right maxillary sinus.

4. Discussion

This study clearly demonstrates the benefits of 3D imaging approach using SPECT/CT compared to planar gamma scintigraphy to assess aerosol sinus deposition in comparison to maxillary sinus lavage reference method. ROIs definition with the 2D methodology, based on anatomical means although inter-subject anatomical differences, appears unsatisfactory and the anatomical regions are not well-defined compared to CT datas available using the 3D approach. Finally results obtained with 2D imaging clearly demonstrate an overestimation of the intrasinus aerosol deposition compared to SPECT-CT 3D imaging. Indeed in 2D there is a clear difficulty for anatomical localization. Due to the low activity obtained in the maxillary sinuses compared to the strong activity in the nasal central cavity, a small error on ROI definition cause an important overestimation of maxillary sinuses deposition.

As a matter of fact, the SPECT/CT methodology allows a precise anatomical definition of the ROI in 3D for the different region of interest (central nasal cavity, maxillary sinuses, ethmoid sinuses and frontal sinuses). The use of combined SPECT-CT scanning

clearly has some important advantages over planar gamma scintigraphy imaging. It was the only powerful nuclear medicine imaging method to accurately assess the aerosol deposition in ENT regions such as the maxillary sinuses. 3D radionuclide imaging combined with anatomical information from CT and computer analysis should become the new reference approach for applications requiring the assessment of regional aerosol deposition. This quantification methodology appears especially useful in avoiding overestimation of sinusal aerosol deposition compared to usual 2D imaging. However SPECT/CT is not without disadvantages. A main limitation involves a higher radiation dose because of the addition of CT. Taking into account our CT parameters, it corresponds to 1.66 mGy CTDi vol (computed tomography dose index volumic). CT add only 0.09 mSv to a planar scintigraphy (39 mGy*cm for the entire head). The head is less radiosensitive than other organs such as lungs. Moreover SPECT/CT also requires a longer acquisition time. However a plastinated model do not have the same disadvantages as healthy volunteers and the results are more reproducible.

Secondly SPECT/CT seems to be the nuclear imaging method most predictive of sinusal active substance deposition. Indeed, the SPECT/CT results are in excellent agreement with the radioactivity quantification of maxillary sinus lavage. A mean of 0.03 ± 0.004% was obtained for SPECT/CT and 0.03 ± 0.02% for the rinsing method (in terms of percentage of the radioactive amount introduced initially in the NL11S nebulizer). Moreover the SPECT/CT results were also quite relevant to results obtained for gentamicin maxillary sinus lavage performed in a previous study (Durand et al., 2012). It was demonstrated that a mean mass of 3.31 µg of antibiotic were deposited in the maxillary sinuses of the same nasal cast using the NL11 device. In terms of percentage of the amount of gentamicin introduced initially into the nebulizer, this result corresponds to 0,001%. All things considered, using a same nasal cast and nebulizer, we proved that the Tc-DTPA sinusal deposition measured by SPECT-CT

overestimates ten times the gentamicin deposition (0.03 ± 0.004%), whereas the Tc-DTPA deposition measured by 2D scintigraphy overestimates a hundred times the gentamicin deposition (0.1 ± 0.1%). Thus, SPECT/CT appeared as the most predictive nuclear medicine technique to assess antibiotic sinusal deposition. However, the quantification deviation between SPECT-CT and gentamicin maxillary sinus lavage could be due to the structural differences of the markers used, on the one hand gentamicin (an aminoside) and on the other hand a radioactive molecule (Tc-DTPA). However SPECT/CT seems to be an efficient methodology of predicting an active substance deposition by aerosoltherapy even with a ten times overestimation which is better than 2D scintigraphy.

Finally the last part of this study employed this innovative SPECT/CT methodology to describe the nasal and sinusal deposition of different aerosol sizes (micrometric *vs.* nanometric). This study clearly demonstrates that 230 nm aerosolized particles with a nasal jet nebulizer are not efficiently deposited in the central nasal cavity (under 2% of the initial charge). Micrometric particles (2.8 µm), on the contrary, are efficiently deposited in the central nasal cavity (30% of the initial charge). Moreover the addition of a 100 Hz acoustic airflow to the 2.8 µm aerosol significantly enhance the deposition in maxillary sinuses which represent a high interest for sinusitis pathologies treatment.

5. Conclusion

SPECT/CT seems to be an efficient methodology for the prediction of sinusal deposition of an active substance by nebulization. Sensibility of the radioactivity detection and efficiency of the SPECT/CT imaging allow us to emphasize the aerosol size dependence of the deposition in different ENT regions. Compared to planar scintigraphy, benefits of SPECT/CT for the assessment of radiolabelled aerosol deposition in rhinology are clearly demonstrated. This 3D methodology should be preferentially used for scintigraphic imaging of sinusal deposition in

Human. Moreover, nebulizers generating micro-sized aerosol (2.8 µm) coupled with a 100 Hz acoustic airflow appear efficient when targeting maxillary sinuses.

Acknowledgements

The authors would like to acknowledge the financial support of the Regional French Association for Aid to Chronic Respiratory Failure Patients (ARAIR), Saint-Etienne Métropole and the Conseil Général de la Loire.

Conflict of interest

Marc Durand is a scientific consultant for DTF society.

Laurent Vecellio and Sandrine Le Guellec are employees of the DTF company.

References

Baroody, F.M. (2007). Mucociliary transport in chronic rhinosinusitis. Clin. Allergy Immunol. *20*, 103–119.

Booker, R. (2009). Interpretation and evaluation of pulmonary function tests. Nurs. Stand. R. Coll. Nurs. Gt. Br. 1987 *23*, 46–56; quiz 58.

Costantino, H.R., Illum, L., Brandt, G., Johnson, P.H., and Quay, S.C. (2007). Intranasal delivery: Physicochemical and therapeutic aspects. Int. J. Pharm. *337*, 1–24.

Criée, C.P., Sorichter, S., Smith, H.J., Kardos, P., Merget, R., Heise, D., Berdel, D., Köhler, D., Magnussen, H., Marek, W., et al. (2011). Body plethysmography – Its principles and clinical use. Respir. Med. *105*, 959–971.

Croce, C., Fodil, R., Durand, M., Sbirlea-Apiou, G., Caillibotte, G., Papon, J.-F., Blondeau, J.-R., Coste, A., Isabey, D., and Louis, B. (2006). In vitro experiments and numerical simulations of airflow in realistic nasal airway geometry. Ann. Biomed. Eng. *34*, 997–1007.

Durand, M., Rusch, P., Granjon, D., Chantrel, G., Prades, J.M., Dubois, F., Esteve, D., Pouget, J.F., and Martin, C. (2001). Preliminary study of the deposition of aerosol in the maxillary sinuses using a plastinated model. J. Aerosol Med. Off. J. Int. Soc. Aerosols Med. *14*, 83–93.

Durand, M., Pourchez, J., Louis, B., Pouget, J.F., Isabey, D., Coste, A., Prades, J.M., Rusch, P., and Cottier, M. (2011a). Plastinated nasal model: a new concept of anatomically realistic cast. Rhinology *49*, 30–36.

Durand, M., Pourchez, J., Aubert, G., Le Guellec, S., Navarro, L., Forest, V., Rusch, P., and Cottier, M. (2011b). Impact of acoustic airflow nebulization on intrasinus drug deposition of a human plastinated nasal cast: new insights into the mechanisms involved. Int. J. Pharm. *421*, 63–71.

Durand, M., Le Guellec, S., Pourchez, J., Dubois, F., Aubert, G., Chantrel, G., Vecellio, L., Hupin, C., De Gersem, R., Reychler, G., et al. (2012). Sonic aerosol therapy to target maxillary sinuses. Eur. Ann. Otorhinolaryngol. Head Neck Dis. *129*, 244–250.

Eberl, S., Chan, H.K., Daviskas, E., Constable, C., and Young, I. (2001). Aerosol deposition and clearance measurement: a novel technique using dynamic SPET. Eur. J. Nucl. Med. *28*, 1365–1372.

Eberl, S., Chan, H.-K., and Daviskas, E. (2006). SPECT Imaging for Radioaerosol Deposition and Clearance Studies. J. Aerosol Med. Off. J. Int. Soc. Aerosols Med. *19*, 8–20.

Fleming, J., Conway, J., Majoral, C., Tossici-Bolt, L., Katz, I., Caillibotte, G., Perchet, D., Pichelin, M., Muellinger, B., Martonen, T., et al. (2011). The use of combined single photon emission computed tomography and X-ray computed tomography to assess the fate of inhaled aerosol. J. Aerosol Med. Pulm. Drug Deliv. *24*, 49–60.

Flesch, J.D., and Dine, C.J. (2012). Lung volumes: Measurement, clinical use, and coding. CHEST J. *142*, 506–510.

Fokkens, W.J., Lund, V.J., Mullol, J., Bachert, C., Alobid, I., Baroody, F., Cohen, N., Cervin, A., Douglas, R., Gevaert, P., et al. (2012). European Position Paper on Rhinosinusitis and Nasal Polyps 2012. Rhinol. Suppl. 3 p preceding table of contents, 1–298.

King, G.G. (2011). Current and emerging imaging in relation to drug discovery in airways disease. Pulm. Pharmacol. Ther. *24*, 497–504.

Laube, B.L. (2007). Devices for aerosol delivery to treat sinusitis. J. Aerosol Med. Off. J. Int. Soc. Aerosols Med. *20 Suppl 1*, S5–17; discussion S17–18.

Moller, W., Saba, G.K., Haussinger, K., Becker, S., Keller, M., and Schuschnig, U. (2011). Nasally inhaled pulsating aerosols: lung, sinus and nose deposition. Rhinology *49*, 286–291.

Möller, W., Schuschnig, U., Meyer, G., Mentzel, H., and Keller, M. (2008). Ventilation and drug delivery to the paranasal sinuses: studies in a nasal cast using pulsating airflow. Rhinology *46*, 213–220.

Möller, W., Münzing, W., and Canis, M. (2010a). Clinical potential of pulsating aerosol for sinus drug delivery. Expert Opin. Drug Deliv. *7*, 1239–1245.

Möller, W., Schuschnig, U., Khadem Saba, G., Meyer, G., Junge-Hülsing, B., Keller, M., and Häussinger, K. (2010b). Pulsating aerosols for drug delivery to the sinuses in healthy volunteers. Otolaryngol.--Head Neck Surg. Off. J. Am. Acad. Otolaryngol.-Head Neck Surg. *142*, 382–388.

Möller, W., Lübbers, C., Münzing, W., and Canis, M. (2011). Pulsating airflow and drug delivery to paranasal sinuses. Curr. Opin. Otolaryngol. Head Neck Surg. *19*, 48–53.

Vecellio, L., De Gersem, R., Le Guellec, S., Reychler, G., Pitance, L., Le Pennec, D., Diot, P., Chantrel, G., Bonfils, P., and Jamar, F. (2011). Deposition of aerosols delivered by nasal route with jet and mesh nebulizers. Int. J. Pharm. *407*, 87–94.

Authors contributions

JP, MD, LL contributed to the conception and the design of research.

LL, JP, NP, SLG, LV and MD materially participated in the research experiments analysis and interpretation of data.

LL and JP were involved with drafting article.

LL, JP, NP, LV, MD materially participated in article preparation.

LV, MC and MD and all others were involved with reviewing the article.

All authors have approved the final version of this article.

		Aerosol deposition		Reference
		2D imaging	*3D imaging (SPECT-CT)*	*in situ rinsing method*
NL11S 2.8 µm	Central nasal cavity	3.2 ± 0.3	2.38 ± 0.3	
	Ethmoid	0.5 ± 0.1	0.03 ± 0.01	
	Maxillary sinuses	0.1 ± 0.1	0.03 ± 0.004	0.03 ± 0.02

Table I: Deposited fractions for the 2D and 3D approaches compared to the *in situ* rinsing method after nebulization with NL11S (2.8 µm). Results are expressed in terms of percentage of the radioactive amount introduced initially into the nebulizer (mean ± SD).

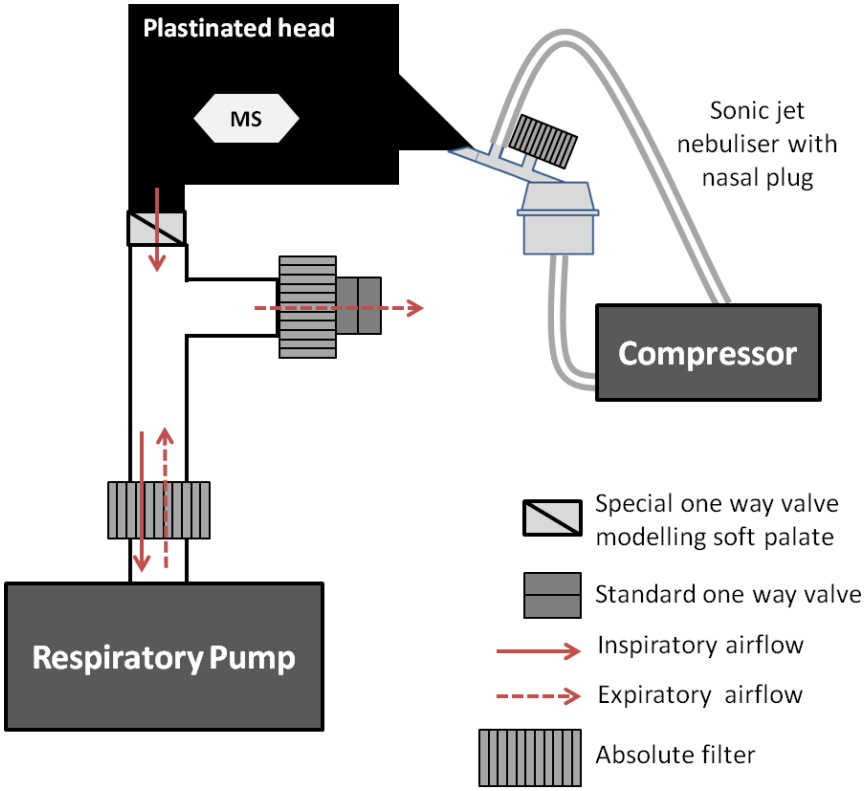

Figure 1: Schematical experimental set-up for nebulization simulating an inspiration by the nose and exhalation trough the mouth thanks to the respiratory pump.

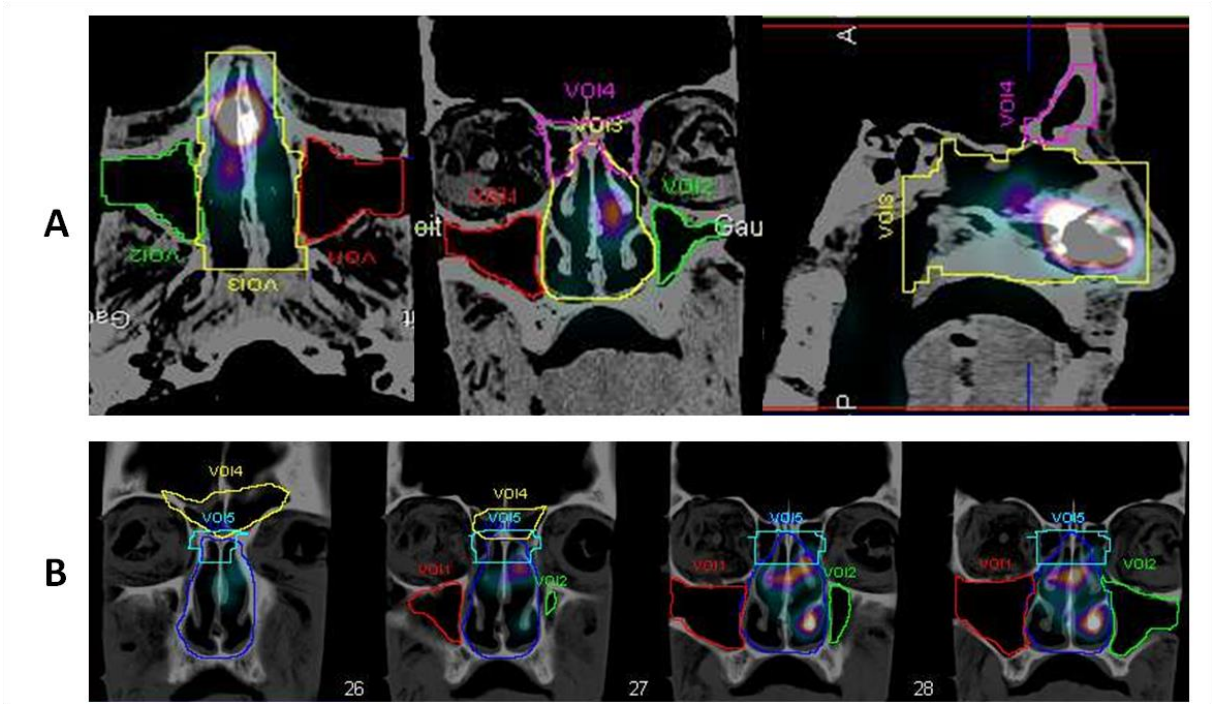

Figure 2: Definition of the 3D imaging anatomical ROIs.

(A) ROI determined by CT scans with radioactivity visualization by SPECT: maxillary sinuses (red and green), central nasal cavity (yellow) and frontal sinuses (purple).

(B) Ethmoid sinuses delimitations (bright blue), maxillary sinuses (red and green), central nasal cavity (dark blue) and frontal sinuses (yellow).

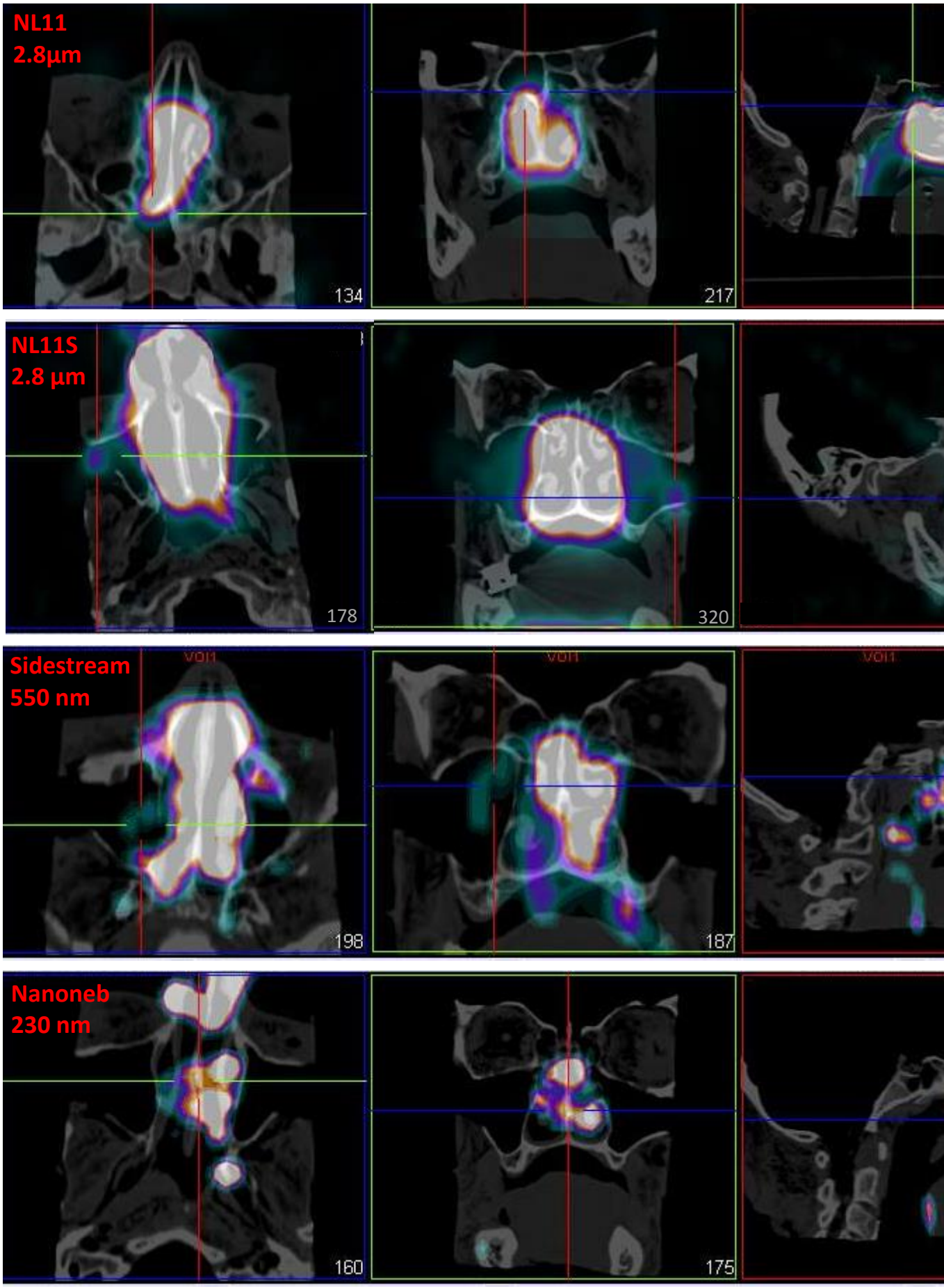
NL11
2.8µm
134
217
NL11S
2.8 µm
178
320
Sidestream
550 nm
198
187
Nanoneb
230 nm
160
175

Figure 3: Illustrative SPECT/CT fused images obtained for each size of aerosol (different type of nebulizer): 2.8 µm (NL11 or NL11S), 550 nm (Sidestream) and 230 nm (Nanoneb).

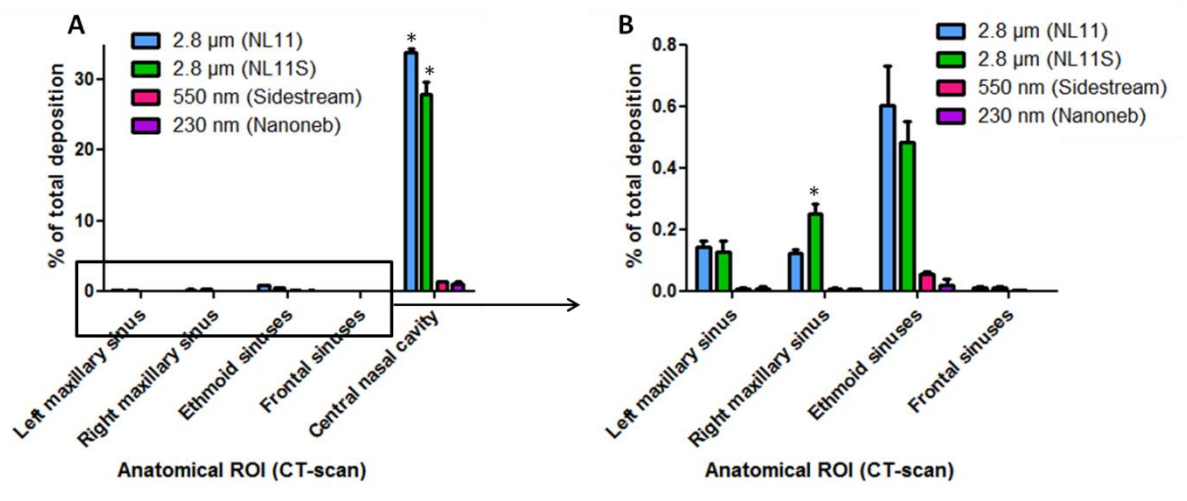

Figure 4: A) Aerosol deposition profile expressed in percentage of total deposition for each size of aerosol (different type of nebulizer) in the different anatomical region of interest (Left and right maxillary sinuses, ethmoid and frontal sinuses and central nasal cavity). The 2.8 µm NL11S condition corresponds to the addition of a 100 Hz acoustic airflow during nebulization. B) is an enlargement on the sinuses data.

A

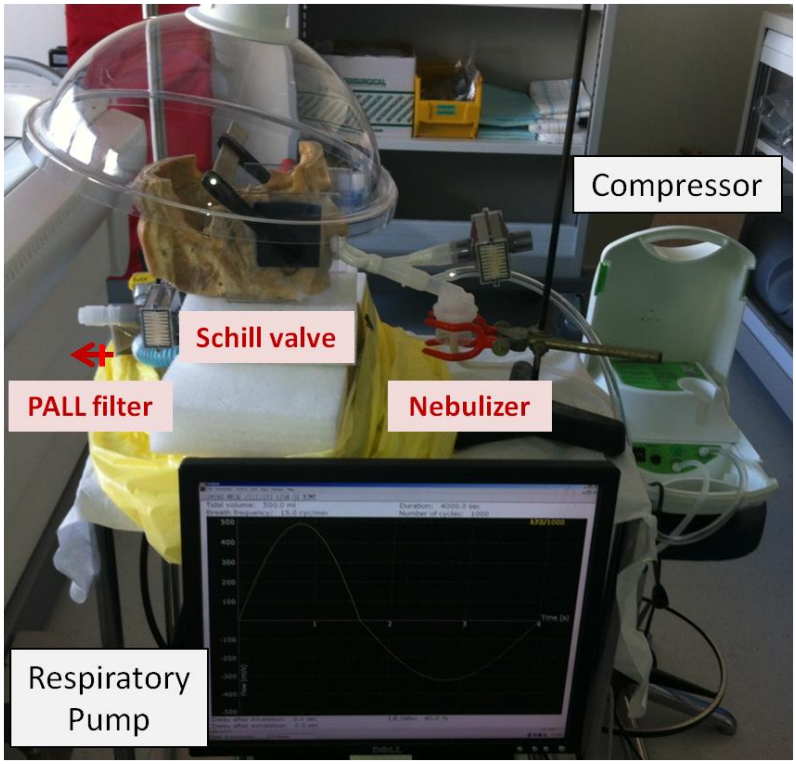

B

Supplementary Information: Experimental set-up for nebulization. A and B corresponds to photography of the set-up in the Nuclear Medicin department (CHU Saint-Etienne).